
PAIRWISE MARKOV CHAINS FOR VOLATILITY FORECASTING

Elie Azeraf, PhD
azerafelie@gmail

ABSTRACT

The Pairwise Markov Chain (PMC) is a probabilistic graphical model extending the well-known Hidden Markov Model. This model, although highly effective for many tasks, has been scarcely utilized for continuous value prediction. This is mainly due to the issue of modeling observations inherent in generative probabilistic models. In this paper, we introduce a new algorithm for prediction with the PMC. On the one hand, this algorithm allows circumventing the feature problem, thus fully exploiting the capabilities of the PMC. On the other hand, it enables the PMC to extend any predictive model by introducing hidden states, updated at each time step, and allowing the introduction of non-stationarity for any model. We apply the PMC with its new algorithm for volatility forecasting, which we compare to the highly popular GARCH(1,1) and feedforward neural models across numerous pairs. This is particularly relevant given the regime changes that we can observe in volatility. For each scenario, our algorithm enhances the performance of the extended model, demonstrating the value of our approach.

Keywords Volatility Forecasting · Pairwise Markov Chain

1 Introduction

Market volatility [1] is one of the most crucial concepts in finance. This notion, capturing stock fluctuations, is pivotal across various financial applications including options pricing, portfolio management, and risk management [2]. For example, volatility is used to price options with the Black-Scholes [3] formulae, and it is primordial on the outcome obtained. Therefore, given its central role in the world of financial engineering, reliably predicting volatility is of paramount importance and can benefit all actors in the financial industry.

There exist numerous ways to define it. Considering the stock 1-minute open prices S_t and T as the number of minutes, in this paper, we use the following formula corresponding to Historic Volatility:[4]:

$$\sigma_t^2 = \sqrt{\frac{1}{T} \sum_{\tau=(t-1) \times T}^{t \times T} u_\tau^2}.$$

Here, u_τ represents the 1-minute log-return, defined as $u_\tau = \log\left(\frac{S_{\tau+1}}{S_\tau}\right)$.

A well-known model for dealing with this concept is the GARCH(1, 1) [5], introduced in 1986, which allows for its assessment, analysis, and prediction. Since then, a vast number of models have tackled this task, such as extensions of the GARCH model [6, 7], neural network-based models [8, 9, 10, 11], or those based on probabilistic graphical models like the Hidden Markov Chain (HMC) [12, 13], also known as the Hidden Markov Model.

In this project, we introduce a novel approach to forecast volatility using the Pairwise Markov Chain (PMC) model [14]. This model, a probabilistic graphical model expanding on the HMC, has rarely been employed for time series prediction [15]. This limited usage is attributed to the difficulty in handling the features of observed variables [16, 17], a problem that we will describe in detail in the next section, and for which we will propose a solution.

Our contribution lies in presenting a new algorithm tailored for time series prediction utilizing the PMC model, capable of handling observations’ features without constraints. Unlike conventional prediction algorithms, our approach extends beyond mere forecasting by integrating hidden states into any prediction model. Specifically, the PMC- f model enables dynamic adjustment of the parameters of a given forecasting model f based on the observed time series and its underlying properties.

The main contributions of our paper are the following:

- (i) We develop a new algorithm for PMC forecasting, allowing the use of PMC without feature constraints.
- (ii) We demonstrate how the PMC extends any forecasting model for time series prediction.
- (iii) We establish the empirical superiority of PMC for volatility forecasting using this new methodology.

This article is organized as follows: First, the next section provides a literature review, presenting the main models for volatility forecasting and detailing the Pairwise Markov Chain. Section 3 is devoted to our main contribution, presenting the new prediction algorithm using PMC, followed by Section 4, which presents empirical results on volatility for different pairs. Finally, our paper concludes with a discussion and conclusion.

2 Theoretical Framework

2.1 Main models for volatility forecasting

The most popular model for processing and predicting volatility is the GARCH(1, 1) model [5]. Given the log-return at time t , u_t , and the volatility at time t , σ_t^2 , it models the next volatility σ_{t+1}^2 as follows:

$$\sigma_{t+1}^2 = \omega + \alpha u_t^2 + \beta \sigma_t^2 + \epsilon_{t+1} \quad (1)$$

with ϵ_{t+1} being a random variable with zero mean, and (α, β, ω) representing the model’s parameters of interest.

Therefore, forecasting with GARCH(1, 1) involves computing

$$\mathbb{E}[\sigma_{t+1}^2] = \omega + \alpha u_t^2 + \beta \sigma_t^2 \quad (2)$$

It can be viewed as a linear combination of the input data to produce a unique output.

This model has been widely extended to incorporate additional features, such as the EGARCH [6], GARCH-M [7], and several other models, enhancing its predictive capabilities [18, 19, 20, 21, 22, 23, 24].

Another widely used family of models for this task is neural network-based ones [25, 26], with studies covering various neural architectures [8, 9, 10, 11]. For our work, we focus on the Feedforward Neural Network (FNN), which comprises a succession of linear combinations followed by non-linear functions, called activation functions. The input data are referred to as the input layer, the returned data as the output layer, and the intermediate variables resulting from linear combinations and activation functions as the hidden layers.

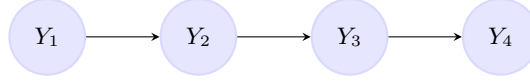


Figure 1: Oriented Probabilistic Graph of the Markov Chain.

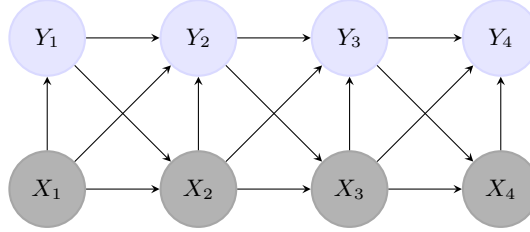


Figure 2: Oriented Probabilistic Graph of the Pairwise Markov Chain.

Given t , for our actual work, we consider the volatility σ_t^2 and the squared log-return u_t^2 as the input layer, and we use three different FNNs:

- FNN(2): composed of the input layer of dimension 2 for our case, a hidden layer of dimension 2, and the output layer, which is of dimension 1 in our case.
- FNN(3): composed of the input layer, a hidden layer of dimension 3, and the output layer.
- FNN(2, 3): composed of the input layer, two hidden layers of dimension 3, and the output layer.

We use the hyperbolic tangent as activation functions. As we aim to predict a continuous random variable, our FNNs do not conclude with an activation function in the output layer.

All the models presented in this subsection model σ_{t+1}^2 as a function of σ_t^2 and u_t^2 , and assume that:

$$\sigma_{t+1}^2 = f(\sigma_t^2, u_t^2) + \epsilon_t, \quad (3)$$

where f is a model and ϵ_t is a random variable with mean equal to 0 and independent from the other random variables. We consider the random variable Y_t taking its values in \mathbb{R}^2 such that the realization y_t of Y_t is (σ_{t+1}^2, u_t^2) . With each model presented in this subsection, the observed process $Y_{1:T} = (Y_1, \dots, Y_T)$ forms a Markov chain, and its probabilistic graph is represented in figure 1.

2.2 The Pairwise Markov Chain model

2.2.1 Definition

The Pairwise Markov Chain (PMC) [14] is a probabilistic graphical model that extends the well-known HMC [27, 28, 29, 30], improving its performance in many fields [17, 31, 32]. It considers the hidden random sequence $X_{1:T} = (X_1, \dots, X_T)$, where X_t takes its value in Λ_X , and the observed sequence $Y_{1:T} = (Y_1, \dots, Y_T)$, where Y_t takes its value in Ω_Y . For this work, we consider $\Lambda_X = (\lambda_1, \dots, \lambda_N)$ as a finite discrete set, and $\Omega_Y = \mathbb{R}^d$, where $d \geq 1$. We also consider a homogeneous PMC, meaning that the laws defining it do not depend on t . The PMC defines the distribution of $(X_{1:T}, Y_{1:T})$ as follows:

$$p(x_{1:T}, y_{1:T}) = p(x_1, y_1) \prod_{t=1}^{T-1} p(x_{t+1}, y_{t+1} | x_t, y_t). \quad (4)$$

Its probabilistic graph is depicted in figure 2. As one can observe, it extends the model shown in figure 1 by adding a hidden process.

Remark Considering the same random variables, the probabilistic law of the HMC is:

$$p(x_{1:T}, y_{1:T}) = p(x_1) \prod_{t=1}^{T-1} p(x_{t+1} | x_t) \prod_{t=1}^T p(y_t | x_t), \quad (5)$$

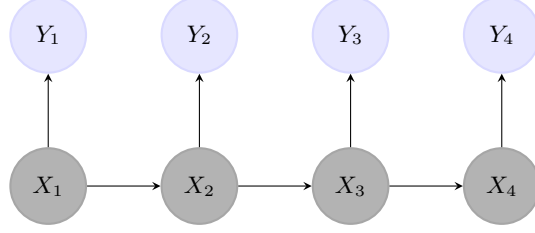


Figure 3: Oriented Probabilistic Graph of the Hidden Markov Chain.

and its graph is in figure 3. Therefore, we see that the PMC is a HMC if and only if $p(x_{t+1}, y_{t+1}|x_t, y_t) = p(x_{t+1}|x_t)p(y_{t+1}|x_{t+1})$.

2.2.2 Usual Forecasting Algorithm

Given $y_{1:t}$, forecasting with the PMC model involves computing $\mathbb{E}[y_{t+1}|y_{1:t}]$. This value is typically computed as follows:

$$\begin{aligned} \mathbb{E}[y_{t+1}|y_{1:t}] &= \mathbb{E}[\mathbb{E}[x_t, x_{t+1}, y_{t+1}|y_{1:t}]] \\ &= \sum_{x_t} \sum_{x_{t+1}} p(x_t, x_{t+1}|y_{1:t}) \mathbb{E}[y_{t+1}|x_t, y_t, x_{t+1}] \\ &= \sum_{x_t} \sum_{x_{t+1}} p(x_t|y_{1:t}) p(x_{t+1}|x_t, y_t) \mathbb{E}[y_{t+1}|x_t, y_t, x_{t+1}]. \end{aligned}$$

$p(x_t|y_{1:t})$ is computed using the Bayes' law:

$$p(x_t|y_{1:t}) = \frac{p(x_t, y_{1:t})}{\sum_{x'_t} p(x'_t, y_{1:t})},$$

computing $p(x_t, y_{1:t})$ recursively:

- For $t = 1$:

$$p(x_1, y_1) = p(x_1)p(y_1|x_1)$$

- For $t > 1$:

$$\begin{aligned} p(x_{t+1}, y_{1:t+1}) &= \sum_{x_t} p(x_t, y_{1:t}, x_{t+1}, y_{t+1}) \\ &= \sum_{x_t} p(x_t, y_{1:t}) p(x_{t+1}|x_t, y_t) p(y_{t+1}|x_t, y_t, x_{t+1}). \end{aligned}$$

Therefore, to apply this algorithm, one needs, for all t , $p(x_t)$, $p(y_t|x_t)$, $p(x_{t+1}|x_t, y_t)$, and $p(y_{t+1}|x_t, y_t, x_{t+1})$. Since we do not observe the hidden sequence $x_{1:T}$ in the training set, the Expectation-Maximization algorithm [33] can be used to learn these parameters.

2.2.3 Handling observations' features

Using the above algorithm, one encounters a well-established problem inherent in algorithms that need to learn the law of observations, as may be the case with probabilistic generative models. Indeed, we have to learn two observation laws: $p(y_t|x_t)$ and $p(y_{t+1}|x_t, y_t, x_{t+1})$.

First, we must assume the law. Although a Gaussian distribution is commonly assumed for its generality and computational simplicity, the actual nature of the distribution may differ significantly

Moreover, the number of parameters is also a problem. If we assume $p(y_t|x_t)$ follows a Gaussian distribution, we have to learn all the means, implying $d \times N$ parameters, and the variance matrices, with $\frac{d(d+1)}{2} \times N$ parameters, resulting in a quadratic dependence. For large values of d , this implies a very large number of parameters. This leads to computational challenges and increased demand for data, potentially imposing limitations on the feasibility of the algorithm.

Conversely, when focusing on learning laws such as $p(x_t|y_t)$, encountered in discriminative models, and assuming a logistic regression model, the parameterization simplifies significantly. In this case, only $d + 1$ parameters need to be learned. This stark reduction in the number of parameters not only streamlines the learning process but also minimizes the risk of overfitting, particularly in situations where the dimensionality of the data is high. The literature largely describes this problem and compares the benefits of using the latest algorithms [16, 34, 35].

Whereas it was accepted that this problem was encountered with generative models, and discriminative ones should be preferred, recent works show that this is not the case and prove that any generative model can define a classifier without using any observation laws [36]. For example, [37, 38] present the Discriminative Forward-Backward algorithm, allowing the computation of $p(x_t|y_{1:T})$ with the HMC without using observation laws, and significantly improving the results. The same work is done for the Naive Bayes model in [39].

3 Methodology

3.1 New algorithm

In 2.2.2, we have seen that $\mathbb{E}[y_{t+1}|y_{1:t}]$ can be computed using the PMC model as:

$$\mathbb{E}[y_{t+1}|y_{1:t}] = \sum_{x_t} p(x_t|y_{1:t}) \sum_{x_{t+1}} p(x_{t+1}|x_t, y_t) \mathbb{E}[y_{t+1}|x_t, y_t, x_{t+1}]. \quad (6)$$

Proposition 3.1 Our new algorithm consists of computing $p(x_t|y_{1:t})$ in a different way, without relying on any observation laws.

- For $t = 1$:

$p(x_1|y_1)$ is given;

- For $t \geq 1$:

$$p(x_{t+1}|y_{1:t+1}) = \frac{\gamma_{t+1}(x_{t+1})}{\sum_{x'_{t+1}} \gamma_{t+1}(x'_{t+1})} \quad (7)$$

with

$$\gamma_{t+1}(x_{t+1}) = \sum_{x_t} p(x_t|y_{1:t}) \frac{p(x_t|y_t, y_{t+1})}{p(x_t|y_t)} p(x_{t+1}|x_t, y_t, y_{t+1}). \quad (8)$$

Thus, computing $\mathbb{E}[y_{t+1}|y_{1:t}]$ never relies on observation laws, allowing PMC to be used for forecasting while avoiding the feature problem.

Proof: First, we express the probability $p(x_{t+1}, y_{1:t+1})$ as follows:

$$\begin{aligned}
 p(x_{t+1}, y_{1:t+1}) &= \sum_{x_t} p(x_t, x_{t+1}, y_{1:t}, y_{t+1}) \\
 &= p(y_{1:t}) \sum_{x_t} p(x_t|y_{1:t}) p(y_{t+1}|x_t, y_t) p(x_{t+1}|x_t, y_t, y_{t+1}) \\
 &= p(y_{1:t}) \sum_{x_t} p(x_t|y_{1:t}) \frac{p(x_t, y_t, y_{t+1})}{p(x_t, y_t)} p(x_{t+1}|x_t, y_t, y_{t+1}) \\
 &= p(y_{1:t}) p(y_{t+1}|y_t) \sum_{x_t} p(x_t|y_{1:t}) \frac{p(x_t|y_t, y_{t+1})}{p(x_t|y_t)} p(x_{t+1}|x_t, y_t, y_{t+1}) \\
 &= p(y_{1:t}) p(y_{t+1}|y_t) \gamma_{t+1}(x_{t+1}).
 \end{aligned}$$

Therefore,

$$p(x_{t+1}|y_{1:t+1}) = \frac{p(x_{t+1}, y_{1:t+1})}{\sum_{x'_{t+1}} p(x'_{t+1}, y_{1:t+1})} = \frac{\gamma_{t+1}(x_{t+1})}{\sum_{x'_{t+1}} \gamma_{t+1}(x'_{t+1})},$$

ending the proof.

Remark 3.1 From the Proposition below, we can deduce the same algorithm for the HMC:

$$\mathbb{E}[y_{t+1}|y_{1:t}] = \sum_{x_t} p(x_t|y_{1:t}) \sum_{x_{t+1}} p(x_{t+1}|x_t) \mathbb{E}[y_{t+1}|x_{t+1}],$$

with

$$\begin{aligned}
 &p(x_1|y_1) \text{ is given;} \\
 p(x_{t+1}|y_{1:t+1}) &= \frac{\delta_{t+1}(x_{t+1})}{\sum_{x'_{t+1}} \delta_{t+1}(x'_{t+1})} \\
 \text{with } \delta_{t+1}(x_{t+1}) &= \sum_{x_t} p(x_t|y_{1:t}) \frac{p(x_{t+1}|x_t)}{p(x_{t+1})} p(x_{t+1}|y_{t+1}).
 \end{aligned}$$

The proof may be directly deducted from the Proof below.

3.2 How the PMC extends other models

Given a forecasting model such as the GARCH(1, 1), the FNN, or any other, we define $f : \mathbb{R}^d \rightarrow \mathbb{R}^{d'}$ as its function. Therefore, given the observations $y_{1:t}$, we estimate the next observed variable as $\hat{y}_{t+1} = f(y_t)$. The computing process is illustrated in figure 4a.

With the PMC and its forecasting algorithm described in 3.1, one can write formula 6 as follows without loss of generality:

$$\begin{aligned}
 \mathbb{E}[y_{t+1}|y_{1:t}] &= \sum_{x_t} p(x_t|y_{1:t}) \sum_{x_{t+1}} p(x_{t+1}|x_t, y_t) \mathbb{E}[y_{t+1}|x_t, y_t, x_{t+1}]. \\
 &= \sum_{x_t} p(x_t|y_{1:t}) g(x_t, y_t)
 \end{aligned}$$

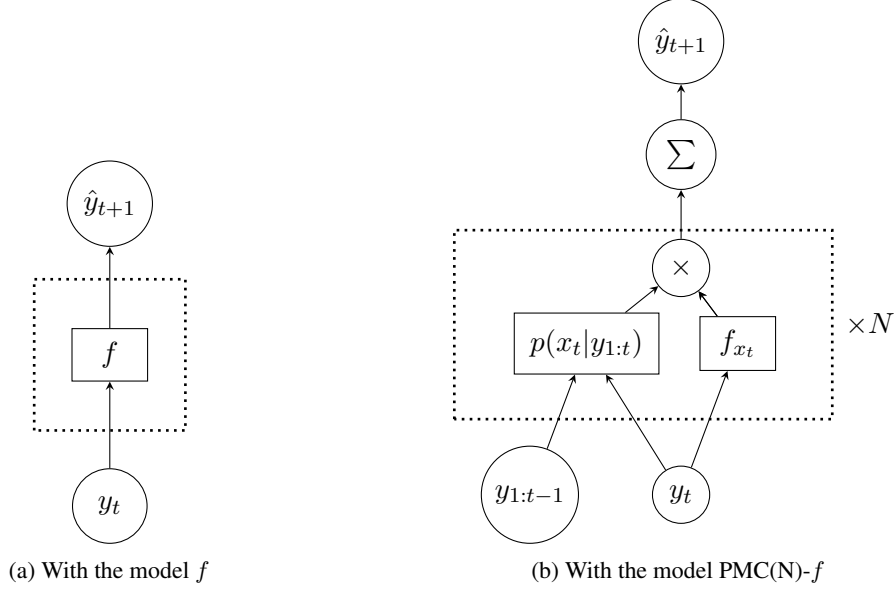


Figure 5: Computing the prediction \hat{y}_{t+1} with the models f and $\text{PMC}(N)-f$.

with $g : \Lambda_X \times \Omega_Y \rightarrow \Omega_Y$. Moreover, one may set $g(x_t, y_t) = f_{x_t}(y_t)$, where f_{x_t} is a function similar to f but with different parameter values. Therefore, with the PMC model having N hidden states and our new algorithm, given N functions f_i similar to the preceding model f , the estimation of the next observed variable is:

$$\hat{y}_{t+1} = \sum_{x_t} p(x_t|y_{1:t}) f_{x_t}(y_t). \quad (9)$$

Therefore, prediction with the PMC can be seen as the weighted average of N models f , where the weights $p(x_t|y_{1:t})$ are calculated based on the entire observed sequence and are computed sequentially with complex dependencies between all the random variables. This computing process is illustrated in figure 4b.

This method offers several benefits:

- The weights at time $t + 1$ differ from those at time t , thanks to the information provided by the new observation at time t ;
- The computation of the weights at time $t + 1$ is fast, depending only on the weights and the observation at time t , thanks to the Markov chain structure;
- This approach generalizes the use of only the model f , as having only one hidden state ($N = 1$) is sufficient to recover the latter. Therefore, we retain the benefits of the initial model, such as the mean-reversion behavior of the GARCH(1, 1), for example.

Remark 3.2. The PMC with our new algorithm and the Regime Switching Models [24, 40] may seem similar, both introducing the notion of hidden states to incorporate non-stationarity. However, our approach is much more general. The Regime Switching Model relies on modeling with far fewer dependencies between random variables, similar to the HMC, sometimes adding a dependency linking the observed random variables. In contrast, the PMC is more general, with more dependencies between the random variables.

4 Results

In this section, we will apply our new PMC algorithm to empirically observe its benefits, depending on base models. For example, we will assess the performance of the GARCH(1, 1) model for volatility forecasting,

PMC for volatility forecasting

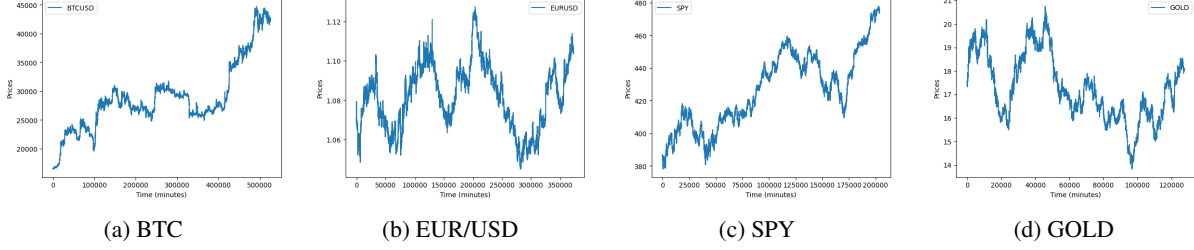


Figure 6: Our four pairs one-minute open-data during 2023.

and then we will combine this model with a PMC having N hidden states, as described in 9, to study the advantages of being able to switch between different states.

In the context of our empirical study, we will use the GARCH(1, 1), the FNN(2), the FNN(3), and the FNN(2, 3) as base models. These models will be combined with PMCs having 2, 3, and 4 hidden states. The model associating the PMC with N hidden states and a model f is denoted PMC(N)- f .

4.1 Data

We focus our empirical study on four different pairs: BTC/USD, EUR/USD, SPY, and GOLD¹. We will apply our algorithms to data throughout the year 2023. The open prices of each pair, with 1-minute intervals, are represented in figure 6.

Our variable of interest, the volatility, is computed over 60-minute intervals. To recall, given the open prices $S_{1:T} = (S_1, \dots, S_T)$, we compute the 1-minute log-returns $u_{1:T} = (u_1, \dots, u_{T-1})$ such that $u_t = \log\left(\frac{S_{t+1}}{S_t}\right)$. Then, we compute volatility data of the stock as follows, for each t :

$$\sigma_t^2 = \sqrt{\frac{1}{60} \sum_{\tau=60(t-1)}^{60t} u_\tau^2}.$$

The volatility data of our four pairs are represented in figure 7.

For each t , our goal is to predict the next volatility σ_{t+1}^2 given the observed volatility sequence $\sigma_{1:t}^2 = (\sigma_1^2, \dots, \sigma_t^2)$ and the observed 60-minute log-returns sequence $u_{1:t}^{(60)} = (u_1^{(60)}, \dots, u_t^{(60)})$, which are squared and computed such that $u_t^{(60)} = \log\left(\frac{S_{60(t+1)}}{S_{60t}}\right)$. For computational purposes, the input and target data are centered and scaled, meaning that their mean is equal to 0 and their variance is equal to 1. Then, they are passed through the logarithm function to reduce discrepancies with outliers. These data are designated as "normalized data".

We evaluate a model's performance using the mean squared error (MSE), which is computed between the ground truth volatility data $\sigma_{1:T}^2$ and the estimated ones $\hat{\sigma}_{1:T}^2$:

$$MSE(\sigma_{1:T}^2, \hat{\sigma}_{1:T}^2) = \frac{1}{T} \sum_{t=1}^T (\sigma_t^2 - \hat{\sigma}_t^2)^2.$$

¹Data may be freely downloaded at <https://polygon.io/>.

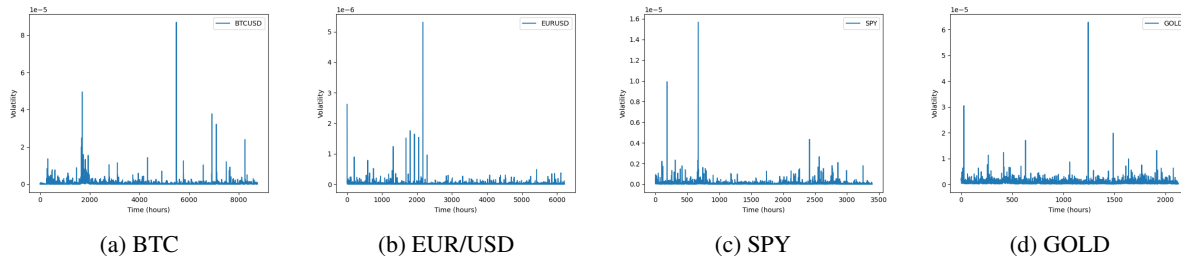


Figure 7: Our four pairs volatility (calculated over each 60-minute interval) during 2023.

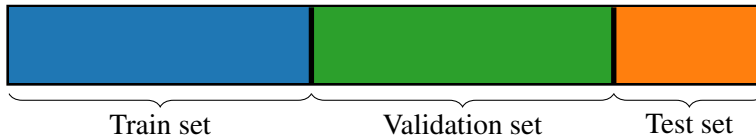


Figure 8: Illustration of the decomposition of the data.

4.2 Training

All the models are trained using the gradient descent algorithm with back-propagation [41, 42]. We utilize the Adam optimizer [43] and the MSE loss function, with a learning rate set to 0.05. In terms of implementation details, all the code is written in Python using the PyTorch [44] library, and the experiments are conducted using a 16GB CPU².

Regarding the PMC-based models, we utilize formula 9 to forecast the next volatility, employing our new algorithm described in 3.1 to compute $p(x_t|y_{1:t})$. Without loss of generality, in 8, we model $\frac{p(x_t|y_t, y_{t+1})}{p(x_t|y_t)}p(x_{t+1}|x_t, y_t, y_{t+1})$ with a neural network function, taking x_t, y_t, x_{t+1} , and y_{t+1} as inputs and producing an output in \mathbb{R}^+ . This simplifies the computation during back-propagation without loss of generality, as it is always possible to define the different probabilities given this function.

A set of parameters is learned for each time series, which is divided into three sets:

- The training set, comprising the first 40% of the data;
- The validation set, comprising 40% of the data in the series, extending up to 80% of it;
- The test set, comprising the remaining data, ranging from 80% of the data to the end of the series.

This decomposition is illustrated in figure 8. Data are not shuffled as we are dealing with temporal data.

4.3 Results

The results of all the models on normalized data are presented in Table 1, and on the original data in Table 2³. All the experiments are reproduced five times, and we report the mean and the Gaussian 95% confidence interval of the MSE. For each model, the best performance, which is the lowest, is highlighted in bold.

5 Discussion

As one may observe, except for a few exceptions, extending a model with the PMC procedure allows for improved performance, as theoretically expected. However, the best performances are not necessarily associated with the highest value of N . This can be explained, in particular, by the overfitting to which we may be subjected during training.

²All the code and experiments are available at https://github.com/ElieAzeraf/Volatility_Prediction_PMC/tree/develop

³For BTC, results have to be multiplied by 10^{-12} , by 10^{-14} for SPY, by 10^{-12} for GOLD, and by 10^{-15} for EURUSD.

	BTC	SPY	GOLD	EURUSD
GARCH(1, 1)	0.337 ± 0.004	0.807 ± 0.014	0.775 ± 0.018	0.625 ± 0.000
PMC(2) - GARCH(1, 1)	0.320 ± 0.003	0.780 ± 0.004	0.655 ± 0.004	0.609 ± 0.005
PMC(3) - GARCH(1, 1)	0.324 ± 0.005	0.791 ± 0.014	0.636 ± 0.013	0.618 ± 0.007
PMC(4) - GARCH(1, 1)	0.321 ± 0.002	0.770 ± 0.011	0.644 ± 0.014	0.616 ± 0.005
FNN(2)	0.331 ± 0.002	0.795 ± 0.004	0.744 ± 0.20	0.620 ± 0.001
PMC(2) - FNN(2)	0.321 ± 0.001	0.779 ± 0.005	0.660 ± 0.19	0.620 ± 0.005
PMC(3) - FNN(2)	0.319 ± 0.002	0.787 ± 0.008	0.618 ± 0.010	0.616 ± 0.005
PMC(4) - FNN(2)	0.321 ± 0.001	0.780 ± 0.006	0.634 ± 0.019	0.616 ± 0.004
FNN(3)	0.335 ± 0.004	0.792 ± 0.007	0.752 ± 0.036	0.622 ± 0.002
PMC(2) - FNN(3)	0.322 ± 0.004	0.778 ± 0.009	0.657 ± 0.026	0.619 ± 0.003
PMC(3) - FNN(3)	0.319 ± 0.003	0.786 ± 0.007	0.625 ± 0.013	0.609 ± 0.004
PMC(4) - FNN(3)	0.320 ± 0.002	0.783 ± 0.002	0.631 ± 0.013	0.612 ± 0.006
FNN(2, 3)	0.333 ± 0.001	0.796 ± 0.009	0.730 ± 0.013	0.623 ± 0.001
PMC(2) - FNN(2, 3)	0.318 ± 0.002	0.775 ± 0.005	0.643 ± 0.014	0.624 ± 0.003
PMC(3) - FNN(2, 3)	0.321 ± 0.002	0.789 ± 0.008	0.639 ± 0.018	0.616 ± 0.005
PMC(4) - FNN(2, 3)	0.320 ± 0.001	0.783 ± 0.007	0.641 ± 0.013	0.614 ± 0.003
HMC(2)	0.341 ± 0.009	0.806 ± 0.016	0.743 ± 0.016	0.624 ± 0.002
HMC(3)	0.331 ± 0.003	0.799 ± 0.007	0.749 ± 0.033	0.624 ± 0.001
HMC(4)	0.328 ± 0.002	0.781 ± 0.009	0.724 ± 0.033	0.624 ± 0.002

Table 1: MSE of the different models for volatility forecasting on normalized data

	BTC	SPY	GOLD	EURUSD
GARCH(1, 1)	1.226 ± 0.019	2.855 ± 0.013	1.350 ± 0.015	1.049 ± 0.000
PMC(2) - GARCH(1, 1)	1.193 ± 0.004	2.893 ± 0.016	1.212 ± 0.016	1.014 ± 0.018
PMC(3) - GARCH(1, 1)	1.205 ± 0.010	2.884 ± 0.014	1.164 ± 0.028	1.034 ± 0.022
PMC(4) - GARCH(1, 1)	1.199 ± 0.009	2.870 ± 0.019	1.197 ± 0.045	1.049 ± 0.008
FNN(2)	1.201 ± 0.002	2.843 ± 0.009	1.310 ± 0.016	1.098 ± 0.001
PMC(2) - FNN(2)	1.198 ± 0.005	2.896 ± 0.025	1.188 ± 0.020	1.087 ± 0.016
PMC(3) - FNN(2)	1.193 ± 0.003	2.881 ± 0.023	1.138 ± 0.016	1.070 ± 0.022
PMC(4) - FNN(2)	1.193 ± 0.003	2.872 ± 0.017	1.156 ± 0.019	1.063 ± 0.004
FNN(3)	1.202 ± 0.004	2.855 ± 0.006	1.296 ± 0.016	1.106 ± 0.009
PMC(2) - FNN(3)	1.196 ± 0.005	2.874 ± 0.013	1.184 ± 0.033	1.097 ± 0.008
PMC(3) - FNN(3)	1.195 ± 0.002	2.851 ± 0.014	1.141 ± 0.019	1.058 ± 0.016
PMC(4) - FNN(3)	1.193 ± 0.002	2.874 ± 0.019	1.158 ± 0.014	1.041 ± 0.038
FNN(2, 3)	1.211 ± 0.010	2.858 ± 0.022	1.321 ± 0.022	1.112 ± 0.008
PMC(2) - FNN(2, 3)	1.193 ± 0.005	2.903 ± 0.038	1.177 ± 0.018	1.186 ± 0.124
PMC(3) - FNN(2, 3)	1.193 ± 0.002	2.888 ± 0.034	1.161 ± 0.019	1.072 ± 0.007
PMC(4) - FNN(2, 3)	1.195 ± 0.002	2.874 ± 0.014	1.155 ± 0.016	1.058 ± 0.017
HMC(2)	1.206 ± 0.005	2.842 ± 0.016	1.335 ± 0.029	1.100 ± 0.003
HMC(3)	1.200 ± 0.003	2.854 ± 0.007	1.285 ± 0.021	1.106 ± 0.004
HMC(4)	1.201 ± 0.004	2.842 ± 0.020	1.283 ± 0.040	1.108 ± 0.003

Table 2: MSE of the models for volatility forecasting (non-normalized data)

The advantage of models based on PMC is always observable on normalized data, as these are raw training data. Regarding non-normalized data, the situation is more nuanced, as the logarithmic transformation can alter the hierarchy of models.

In the context of the results obtained, it is interesting to delve further into the contribution of different states. To illustrate our point, we focus on the comparison between GARCH(1, 1) and PMC(2)-GARCH(1, 1) applied to the BTC data. First, we compare the parameter values. To recall, on the one hand, for the

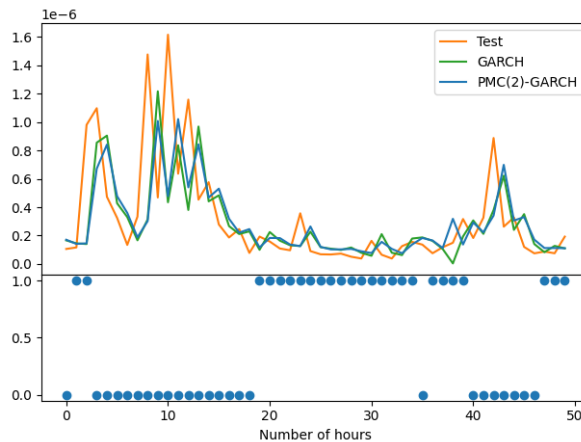


Figure 9: Model predictions with some PMC states

GARCH(1, 1) model, one has the parameters (ω, α, β) . On the other hand, with the PMC(2)-GARCH(1, 1), there are two sets $(\omega_0, \alpha_0, \beta_0)$ and $(\omega_1, \alpha_1, \beta_1)$ from two GARCH(1, 1) models aggregated with 9. In our case, we have the following values:

- $(\omega, \alpha, \beta) = (-0.0155, 0.1674, 0.7221)$;
- $(\omega_0, \alpha_0, \beta_0) = (0.1730, 0.0161, 0.6508)$ and $(\omega_1, \alpha_1, \beta_1) = (-0.3346, -0.0432, 0.4853)$

To illustrate these states, we present some predictions on the test set with the PMC(2)-GARCH(1, 1) in figure 9. From the graph, we can infer that state 0 corresponds to low volatility periods, while state 1 indicates high volatility periods. This deduction aligns with the values of the learned parameters.

6 Conclusion

In this paper, we have developed a new algorithm with the PMC to forecast the next value of a time series. This algorithm is relevant insofar as it allows the introduction of hidden states that make any predictive model non-stationary. Moreover, it does not suffer from the usual features problem of generative models, thanks to a recent methodology described in [36, 38]. Therefore, this new algorithm allows for the improvement of any forecasting model, and we show that empirically with volatility forecasting.

We have applied our new algorithm to volatility forecasting by extending the GARCH(1, 1) model and FNN-based models. As future directions, it might be interesting to extend to other models such as RNNs [45, 46], LSTMs [47], or even XGBoost [48], and apply them to other forecasting tasks.

References

- [1] Robert J Shiller. *Market Volatility*. MIT press, 1992.
- [2] John Hull. *Options, Futures, and Other Derivative Securities*, volume 7. Prentice Hall Englewood Cliffs, NJ, 1993.
- [3] Fischer Black and Myron Scholes. The Pricing of Options and Corporate Liabilities. *Journal of political economy*, 81(3):637–654, 1973.
- [4] Ser-Huang Poon and Clive W J Granger. Forecasting Volatility in Financial Markets: A Review. *Journal of economic literature*, 41(2):478–539, 2003.
- [5] Tim Bollerslev. Generalized Autoregressive Conditional Heteroskedasticity. *Journal of econometrics*, 31(3):307–327, 1986.

- [6] Daniel B Nelson. Conditional Heteroskedasticity in Asset Returns: A New Approach. *Econometrica: Journal of the econometric society*, pages 347–370, 1991.
- [7] Robert F Engle and Tim Bollerslev. Modelling the Persistence of Conditional Variances. *Econometric reviews*, 5(1):1–50, 1986.
- [8] Wenbo Ge, Pooia Lalbakhsh, Leigh Isai, Artem Lenskiy, and Hanna Suominen. Neural Network–Based Financial Volatility Forecasting: A Systematic Review. *ACM Computing Surveys (CSUR)*, 55(1):1–30, 2022.
- [9] Andrea Bucci. Cholesky–ANN Models for Predicting Multivariate Realized Volatility. *Journal of Forecasting*, 39(6):865–876, 2020.
- [10] Andrés Vidal and Werner Kristjanpoller. Gold Volatility Prediction using a CNN-LSTM Approach. *Expert Systems with Applications*, 157:113481, 2020.
- [11] Linyi Yang, Tin Lok James Ng, Barry Smyth, and Rihai Dong. HTML: Hierarchical Transformer-based Multi-task Learning for Volatility Prediction. In *Proceedings of The Web Conference 2020*, pages 441–451, 2020.
- [12] Maciej Augustyniak, Luc Bauwens, and Arnaud Dufays. A new approach to volatility modeling: the factorial hidden markov volatility model. *Journal of Business & Economic Statistics*, 37(4):696–709, 2019.
- [13] Jiawen Luo, Tony Klein, Qiang Ji, and Chenghan Hou. Forecasting realized volatility of agricultural commodity futures with infinite hidden markov har models. *International Journal of Forecasting*, 38(1):51–73, 2022.
- [14] Wojciech Pieczynski. Pairwise Markov Chains. *IEEE Transactions on pattern analysis and machine intelligence*, 25(5):634–639, 2003.
- [15] Marc Escudier, Ikram Abdelkefi, Clément Fernandes, and Wojciech Pieczynski. Forecasting with Pairwise Gaussian Markov Models. *arXiv preprint arXiv:2402.07532*, 2024.
- [16] Andrew Ng and Michael Jordan. On Discriminative vs. Generative Classifiers: A Comparison of Logistic Regression and Naive Bayes. *Advances in neural information processing systems*, 14, 2001.
- [17] Elie Azeraf, Emmanuel Monfrini, Emmanuel Vignon, and Wojciech Pieczynski. Highly Fast Text Segmentation with Pairwise Markov Chains. In *2020 6th IEEE Congress on Information Science and Technology (CiSt)*, pages 361–366. IEEE, 2021.
- [18] Stefan Lundbergh and Timo Teräsvirta. Evaluating GARCH Models. *Journal of Econometrics*, 110(2):417–435, 2002.
- [19] Timo Teräsvirta. An Introduction to Univariate GARCH Models. In *Handbook of financial time series*, pages 17–42. Springer, 2009.
- [20] Luc Bauwens, Sébastien Laurent, and Jeroen VK Rombouts. Multivariate GARCH Models: a Survey. *Journal of applied econometrics*, 21(1):79–109, 2006.
- [21] Christian Francq and Jean-Michel Zakoian. *GARCH Models: Structure, Statistical Inference and Financial Applications*. John Wiley & Sons, 2019.
- [22] Philip Hans Franses and Dick Van Dijk. Forecasting Stock market Volatility using (non-linear) GARCH Models. *Journal of forecasting*, 15(3):229–235, 1996.
- [23] Shiyi Chen, Wolfgang K Härdle, and Kiho Jeong. Forecasting Volatility with Support Vector Machine-based GARCH Model. *Journal of Forecasting*, 29(4):406–433, 2010.
- [24] Franc Klaassen. *Improving GARCH Volatility Forecasts with Regime-Switching GARCH*. Springer, 2002.
- [25] Yann LeCun, Yoshua Bengio, and Geoffrey Hinton. Deep Learning. *nature*, 521(7553):436–444, 2015.
- [26] Ian Goodfellow, Yoshua Bengio, and Aaron Courville. *Deep Learning*. MIT press, 2016.
- [27] Ruslan Leont’evich Stratonovich. Conditional Markov Processes. In *Non-Linear Transformations of Stochastic Processes*, pages 427–453. Elsevier, 1965.

- [28] Leonard E Baum and Ted Petrie. Statistical Inference for Probabilistic Functions of Finite State Markov Chains. *The Annals of Mathematical Statistics*, 37(6):1554–1563, 1966.
- [29] Olivier Cappé, Eric Moulines, and Tobias Rydén. *Inference in Hidden Markov Models*. Springer Science & Business Media, 2006.
- [30] Lawrence Rabiner and B Juang. An Introduction to Hidden Markov Models. *IEEE ASSP Magazine*, 3(1):4–16, 1986.
- [31] Stéphane Derrode and Wojciech Pieczynski. Signal and Image Segmentation using Pairwise Markov Chains. *IEEE Transactions on Signal Processing*, 52(9):2477–2489, 2004.
- [32] Ivan Gorynin, Emmanuel Monfrini, and Wojciech Pieczynski. Pairwise Markov Models for Stock Index Forecasting. In *2017 25th European Signal Processing Conference (EUSIPCO)*, pages 2041–2045. IEEE, 2017.
- [33] Arthur P Dempster, Nan M Laird, and Donald B Rubin. Maximum Likelihood from Incomplete Data via the EM Algorithm. *Journal of the royal statistical society: series B (methodological)*, 39(1):1–22, 1977.
- [34] John D Lafferty, Andrew McCallum, and Fernando CN Pereira. Conditional Random Fields: Probabilistic Models for Segmenting and Labeling Sequence Data. In *Proceedings of the International Conference on Machine Learning*, 2001.
- [35] Andrew McCallum, Dayne Freitag, and Fernando CN Pereira. Maximum Entropy Markov Models for Information Extraction and Segmentation. In *Proceedings of the International Conference on Machine Learning*, volume 17, pages 591–598, 2000.
- [36] Elie Azeraf, Emmanuel Monfrini, and Wojciech Pieczynski. Deriving Discriminative Classifiers from Generative Models. *arXiv preprint arXiv:2201.00844*, 2022.
- [37] Elie Azeraf, Emmanuel Monfrini, Emmanuel Vignon, and Wojciech Pieczynski. Hidden Markov Chains, Entropic Forward-Backward, and Part-of-Speech Tagging. *arXiv preprint arXiv:2005.10629*, 2020.
- [38] Elie Azeraf, Emmanuel Monfrini, and Wojciech Pieczynski. Equivalence between LC-CRF and HMM, and Discriminative Computing of HMM-Based MPM and MAP. *Algorithms*, 16(3):173, 2023.
- [39] Elie Azeraf, Emmanuel Monfrini, and Wojciech Pieczynski. Using the Naive Bayes as a Discriminative Model. In *2021 13th International Conference on Machine Learning and Computing*, pages 106–110, 2021.
- [40] James D Hamilton. Regime Switching Models. In *Macroeconometrics and time series analysis*, pages 202–209. Springer, 2010.
- [41] Yann LeCun, D Touresky, G Hinton, and T Sejnowski. A Theoretical Framework for Back-Propagation. In *Proceedings of the 1988 connectionist models summer school*, volume 1, pages 21–28. San Mateo, CA, USA, 1988.
- [42] Yann LeCun, Bernhard Boser, John S Denker, Donnie Henderson, Richard E Howard, Wayne Hubbard, and Lawrence D Jackel. Backpropagation applied to Handwritten Zip Code Recognition. *Neural computation*, 1(4):541–551, 1989.
- [43] Diederik P Kingma and Jimmy Ba. Adam: A Method for Stochastic Optimization. *arXiv preprint arXiv:1412.6980*, 2014.
- [44] Adam Paszke, Sam Gross, Francisco Massa, Adam Lerer, James Bradbury, Gregory Chanan, Trevor Killeen, Zeming Lin, Natalia Gimelshein, Luca Antiga, et al. PyTorch: An Imperative Style, High-Performance Deep Learning Library. *Advances in neural information processing systems*, 32, 2019.
- [45] David E Rumelhart, Geoffrey E Hinton, and Ronald J Williams. Learning Internal Representations by Error Propagation. Technical report, California Univ San Diego La Jolla Inst for Cognitive Science, 1985.
- [46] Michael I. Jordan. *Attractor Dynamics and Parallelism in a Connectionist Sequential Machine*, page 112–127. IEEE Press, 1990.

- [47] Sepp Hochreiter and Jürgen Schmidhuber. Long Short-Term Memory. *Neural computation*, 9(8):1735–1780, 1997.
- [48] Tianqi Chen and Carlos Guestrin. XGBoost: A Scalable Tree Boosting System. In *Proceedings of the 22nd acm sigkdd international conference on knowledge discovery and data mining*, pages 785–794, 2016.